



1 **Neoglacial trends in diatom dynamics from a small alpine lake in the Qinling**
2 **Mountains of central China.**

3
4 Bo Cheng¹, Jennifer Adams², Jianhui Chen³, Aifeng Zhou³, Qing Zhang³, Anson Mackay^{4*}

5
6 ¹Bo Cheng,
7 College of Urban and Environmental Science, Central China Normal University,
8 Wuhan 430079 China
9 chengbo@mail.ccnu.edu.cn

10
11 ²Jennifer Adams
12 Department of Earth Sciences, University of Toronto, Toronto, ON, Canada
13 j.adams@utoronto.ca

14
15 ³JianHui Chen
16 Key Laboratory of West China's Environmental System (Ministry of Education), College of
17 Earth and Environmental Sciences, Lanzhou University, Lanzhou 730000 China
18 jhchen@lzu.edu.cn

19
20 ³Aifeng Zhou,
21 Key Laboratory of Western China's Environmental Systems (Ministry of Education), College
22 of Earth and Environmental Sciences, Lanzhou University, Lanzhou 730000, China
23 zhouaf@lzu.edu.cn

24
25 ³Qing Zhang,
26 Key Laboratory of Western China's Environmental Systems (Ministry of Education), College
27 of Earth and Environmental Sciences, Lanzhou University, Lanzhou 730000, China
28 Zhangqing16@lzu.edu.cn

29
30 ⁴Anson Mackay*
31 ECRC, Department of Geography, UCL, London WC1E 6BT UK
32 a.mackay@ucl.ac.uk
33 Corresponding Author

34
35
36
37
38



39

40 **Abstract:**

41

42 During the latter stages of the Holocene, and prior to anthropogenic global warming, the
43 Earth underwent a period of cooling called the neoglacial. The neoglacial was associated
44 with declining summer insolation and changes to Earth surface albedo. Although impacts
45 varied globally, in China the neoglacial was generally associated with cooler, more arid
46 climate, which led to renewed permafrost formation, and shifts in vegetation composition.
47 Few studies in central China, however, have explored the impact of neoglacial cooling on
48 freshwater diversity, especially in remote alpine regions. Here we take a palaeolimnological
49 approach to characterise multidecadal variability in diatom community composition, beta-
50 diversity, and flux-inferred productivity over the past 3,500 years in the Qinling Mountains,
51 biodiversity hotspot. We investigate the impact of long-term cooling on primary producers in
52 an alpine lake, which are fundamental to overall aquatic ecosystem function. We show that
53 trends in beta-diversity and shifts in ecological guilds likely reflect changing lake-catchment
54 resource availability, linked to both long-term attenuation of the Asian summer monsoon,
55 and abrupt cool events, linked to a strengthened Siberian High. Important diatom community
56 and productivity responses to the Medieval Climatic Optimum and the Little Ice Age are all
57 apparent in our record, although impact from previous centennial-scale, cool-events are less
58 evident.

59

60 **Keywords:**

61 Diatoms, beta-diversity, Qinling Mountains, neoglacial

62

63



64

65 1. Introduction

66

67 Alpine freshwaters have multiple ecosystem functions (Messerli et al. 2004; Buytaert *et al.*,
68 2017) and provide many ecosystem services such as freshwater regulation and habitat
69 provision (Grêt-Regamey et al. 2011). Their multifunctionality depends on local species
70 assemblages, and how they vary through space and time, i.e. beta-diversity (Mori *et al.*
71 2018). Beta-diversity links biodiversity at regional and local scales, and the amount of
72 compositional change over time can provide important indications about ecosystem
73 functioning (Birks 2007). For example, estimating species turnover assumes that species are
74 lost and gained over time in response to resource availability, competition, historical events
75 and environmental factors such as climate change, over both recent (Smol et al. 2005) and
76 long timescales (Leprieur et al. 2011). However, Alpine regions around the world are some
77 of the most sensitive to changing climate, due in part to elevation-dependent warming (Pepin
78 et al. 2015). Elevation-dependent warming in recent decades across sites on the Tibetan
79 Plateau, for example, showed some of the greatest changes globally (Yan and Liu 2014).
80 Understanding how high altitude ecosystems respond to changing climate is a matter of
81 urgency, because not only do these regions act as ‘water towers’ supplying water to huge
82 populations downstream (Messerli et al. 2004; Buyteart *et al.*, 2017), but their habitats to
83 many iconic species are also vulnerable (e.g. Fan et al. 2014).

84

85 Natural archives are an important resource for reconstructing past environments where long-
86 term records are either scarce or absent. In central China, speleothems provide exceptional,
87 high resolution records of monsoon intensity, allowing periods of multiannual and
88 multidecadal drought to be determined (Wang et al. 2005). Yet there are relatively few
89 studies (e.g. Liu et al. 2017) which have explored multidecadal records of biodiversity
90 change over similar timescales, leaving a fundamental gap in understanding as to how
91 biodiversity in freshwater ecosystems, especially at higher altitudes, responded to periods of



92 climate variability. Reconstructing the impacts of past climate on freshwater ecosystems is
93 fundamental to understanding how freshwater biodiversity may respond to future climate,
94 especially during periods of rapid change. Here we focus on the neoglacial, which spans at
95 least the past c. 3,500 years.

96

97 The neoglacial, characterised by increasingly cooler temperatures, follows on from global
98 warmth of the early- to mid-Holocene. The extent of cooling varied regionally; it was very
99 pronounced in the extra-tropical northern hemisphere, but was less monotonic at low
100 latitudes (Marcott et al. 2013). The most important driver of northern hemisphere cooling is
101 declining summer insolation in conjunction with changes in albedo on the Earth's surface,
102 linked to feedbacks from vegetation and snow-ice albedo. In China, the neoglacial resulted
103 in the persistent decline in monsoon intensity in southern China (Wang et al. 2005) and rapid
104 decline in precipitation in northern China (Chen et al. 2015a) leading to increased aridity and
105 major shifts in vegetation communities (Zhou et al. 2010). Superimposed on the insolation-
106 driven neoglacial were notable periods of sub Milankovitch, centennial-scale climatic events
107 (e.g. Mayewski et al. 2004; Mann et al. 2009; Wanner et al. 2014), including the 2,800 yr BP
108 event (Hall et al. 2004), the Medieval Climactic Anomaly (c. 1000-1300 AD) and Little Ice
109 Age (c. 1300 – 1850 AD). The latter two events are well expressed throughout China;
110 Medieval temperatures were generally warmer than the following centuries spanning the LIA
111 (Cook et al. 2013; Chen et al. 2015b). However, while the LIA generally resulted in periods
112 of aridity (e.g. Wang et al. 2005; Tan et al. 2011; Chen et al. 2015a), in depth research
113 highlights a more heterogenous response across China (e.g. Cook et al. 2010), with some
114 central and southern regions becoming wetter due to interplays between the Westerly jet
115 stream and the ASM (Tan et al. 2018).

116

117 Freshwater ecosystems in the Qinling Mountains of central China provide natural capital and
118 ecosystem services for local and regional populations, and understanding the impact of
119 monsoon variability on ecosystem functioning has the potential to add insight into how



120 freshwater biodiversity may respond to future climate change, and predicted increases in
121 mean annual precipitation (Guo et al. 2017). In this study, we investigate the effects of long-
122 term climate change on freshwater biodiversity in an alpine lake situated in the Qinling
123 mountain range, central China. Specifically we reconstruct trends in diatom community
124 composition, their ecological guilds, and compositional turnover (beta-diversity) at a
125 multidecadal resolution (c. 55 yrs) over the past 3500 years, to determine how primary
126 producers have responded to neoglacial climate change and changing resource availability.
127 We hypothesise that neoglacial cooling would result in a decline in available resources, and
128 with it a decline in diatom beta-diversity.

129

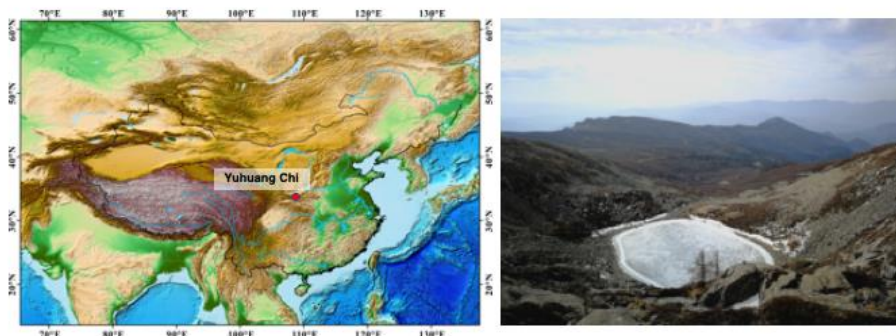
130 **1.1 Study region**

131

132 The Qinling Mountains are widely recognised as a biodiversity hotspot (Fan et al. 2014;
133 Zhang et al. 2017). The region is climatically very sensitive, as it separates the northern
134 subtropical zone of China from the country's central warm-temperate zone (Figure 1).
135 Mount Taibai (34°N, 108°E; 3767 m), is the highest mountain in the range, with a timberline
136 at c. 3,370 m, and treeline at c. 3,600 m (Liu et al. 2002). The mountain is classified as a
137 glacial heritage site because Quaternary glaciations are well preserved, especially the last
138 glaciation (Yang et al. 2018). On Mount Tabai there are several clusters of cirque lakes, and
139 our study site, Lake Yuhuang Chi (YHC), is found in one of these clusters. It is a cirque and
140 moraine lake at 3370 masl, with a maximum depth of 21.5m and an area of c. 23,600 m². Its
141 location places it in the *Larix* forest - subalpine meadow ecotone, making the lake –
142 catchment ecosystem very sensitive to changes in climate.

143

144 **Figure 1:** Regional position of Lake Yuhuang Chi in the Qinling Mountains of central Asia.
145 The lake is situated 3365m asl, and was formed by glacial activity. The photograph of the
146 frozen lake to the right shows the small catchment and tundra vegetation.



147

148

149 2. Methods:

150

151 2.1 Coring, Age model

152 A 135 cm sediment core (YHC15A) was collected using a 6cm diameter piston corer from
153 the central region of Lake Yuhuang Chi. The core consisted entirely of grey-brown gyttja.
154 Radiocarbon dating was carried out on bulk organic sediments using accelerator mass
155 spectrometry (AMS) at Beta Analytic. There is a radiocarbon reservoir effect evident in the
156 data, so we used a quadratic extrapolation to determined reservoir ages. All the radiocarbon
157 dates were quadratic fitted ($^{14}\text{CAge} = 0.0693\text{depth}^2 + 17.31\text{depth} + 1340$, $R^2 = 0.9994$), so
158 we determined the top (0cm) with a 1340 year reservoir age effect. An age-depth model was
159 developed with smooth fit using CLAM 2.2 (Blaauw, 2010) in R, using Intcal13 (Reimer et
160 al., 2013) calibration curve.

161

162 2.2 Diatoms

163 Diatom analysis was performed on alternate sediment samples, at a resolution of c. every 55
164 years. Approximately 0.1g of wet sediment from each sample was prepared using standard
165 procedures. Organic matter was removed by heating each sample in 30% H_2O_2 , before 10%
166 HCl was added to remove carbonates and any excess H_2O_2 . Diatom concentrations were



167 calculated through the addition of divinylbenzene (DVB) microspheres (concentration $8.02 \times$
168 10^5 spheres/cm²) to diatom suspensions, and diatom fluxes calculated using sediment
169 accumulation rates. Diatom suspensions were diluted such that suitable concentrations
170 could be calculated and then pipetted onto coverslips to dry before being fixed onto
171 microscope slides with Naphrax. Using a Zeiss AxioStar Plus light microscope, diatoms were
172 counted at $\times 1000$ magnification under an oil-immersion objective and phase contrast. A
173 minimum of 300 diatom valves were counted for each sample (min 331, max 591). Diatoms
174 were identified using a variety of flora including Krammer and Lange-Bertalot, 1986, 1988,
175 1991a, 1991b; Williams and Round, 1987; Lange-Bertalot, 2001.

176

177 Diatom species were categorised according to ecological guilds commonly associated with
178 the abundance of available resources (e.g. light, nutrients) and disturbance (e.g. grazing)
179 (after Passy 2007; Rimet and Bouchez 2012). The low profile guild includes diatoms which
180 attach themselves to substrates in erect, prostrate, and adnate forms, are very slow moving
181 (Passy 2007), and are generally adapted to low nutrient conditions. High profile guild
182 diatoms are those of tall stature (e.g. they are filamentous, or chain-forming, or found in
183 mucilage tubes), and are generally adapted to high nutrients and low levels of disturbance
184 (Passy 2007). Motile diatoms are relatively fast moving species, tolerant of high nutrients
185 (Passy 2007). A new planktic guild was determined by Rimet and Bouchez (2012) which
186 includes centric species able to resist sedimentation in lake ecosystems.

187

188 **2.3 Multivariate analyses**

189 The magnitude of diatom turnover was initially estimated using detrended correspondence
190 analysis (DCA), with square root transformation of the species data to stabilise variance and
191 rare species downweighted. The axis 1 gradient length was 1.44 standard deviation units, so
192 diatom abundances were reanalysed using principal components analysis (PCA). A log-
193 linear contrast PCA was undertaken, with symmetric scaling of ordination scores so that
194 scaling of both samples and species were optimised. A log-linear contrast PCA was also



195 undertaken for taxa grouped into genera. Beta-diversity, or species compositional change,
196 was estimated using detrended canonical correspondence analyses (DCCA), with the
197 diatom data constrained using dates from the calibrated age model (e.g. see Smol et al.
198 2005). We used DCCA to estimate beta-diversity because sample scores are scaled to be
199 standard units of compositional turnover through the process of detrending by segments and
200 non-linear rescaling (Birks 2007). Sample scores can therefore be interpreted as the amount
201 of species turnover through time, making them ecologically useful and ideal for estimating
202 compositional turnover. Ordinations was undertaken using Canoco5 (Šmilauer and Lepš
203 2014). Breakpoint analysis, a form of segmented regression analysis was used to determine
204 major points of change in diatom composition, beta-diversity using the segmented package
205 in R v. 3.5.1 (Muggeo 2008). Stringent p-values were adopted ($p < 0.001$) when determining
206 any major changes observed. All stratigraphical profiles shown were constructed using C2
207 Data Analysis Version 1.7.2, and zones determined using stratigraphical constrained cluster
208 analysis by incremental sum of squares (CONISS) and broken stick analysis using the rioja
209 package in R v. 3.5.1 (Juggins 2017).
210



211

212 **3. Results**

213

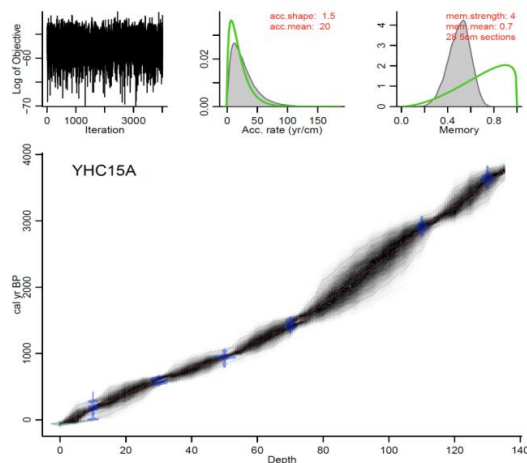
214 **3.1 Age Model**

215 Table 1: AMS-¹⁴C radiocarbon dates from Lake Yuhuang Chi (core YHC15A)

Lab No.	Depth (cm)	Material	δ ¹³ C (‰ VPDB)	¹⁴ C date ±error (yr BP)	¹⁴ C date minus 1340 reservoir age (yr BP)	Weighted calibrated age (No error) (yr BP)
Beta-425231	10	Bulk organic	-24.6	1530±30	190±30	168
Beta-425232	30	Bulk organic	-24.7	1920±30	580±30	595
Beta-425233	50	Bulk organic	-24.9	2370±30	1030±30	949
Beta-417757	70	Bulk organic	-24.8	2870±30	1530±30	1423
Beta-425234	110	Bulk organic	-24.8	4140±30	2800±30	2868
Beta-417758	130	Bulk organic	-24.9	4730±30	3390±30	3584

216

217 **Figure 2:** The age model determined on 5 radiocarbon dates of organic bulk sediments from
 218 core YHC15A. The age-depth model was developed with smooth fitting using CLAM 2.2
 219 (Blaauw, 2010).
 220



221

222



223 3.2 Diatoms

224 A total of 170 species of diatom were identified from Lake Yuhuang Chi, although by far the
225 majority, 120 species, were rare (present < 1%). For much of the past 3,500 years, diatoms
226 were dominated by fragilarioids and naviculoids up to c. 930 cal yrs BP, [1020 CE] after
227 which they decline, to be replaced by monoraphid and *Gomphonema*-type taxa alongside
228 the centric *Puncticulata*. Stratigraphically constrained cluster analysis by incremental sum of
229 squares analyses (CONISS) on diatom relative abundance data reveals three zones. Zone 1
230 (c. 3550 – 2300 cal yrs BP), Zone 2 (c. 2300 – 615 cal yrs BP), and Zone 3 (c. 615 cal yrs
231 BP – present) (Fig 3,4). Zone 1 is dominated by diatoms in the high profile guild (Fig 4),
232 notably fragilarioids *Stauroforma exiguiformis* and *Staurosirella pinnata*. Diatoms in the
233 motile guild are well represented by the naviculoid *Humidophila schmassmannii*, together
234 with *Diademsis gallica*, *Mayamaea atomus* and *Mayamaea fossalis*. The decline in *S.*
235 *exiguiformis* at the top of the zone is accompanied by an increase in *Pseudostaurosira*
236 *brevistriata*, and decline in motile diatoms e.g. *M. atomus*. In Zone 1, there is a gradual
237 decline in beta-diversity, and decline in PCA1 samples scores. Zone 2 is marked by a
238 notable increase in the planktic *Puncticulata bodanica* and increasing *P. brevistriata* and
239 *Pseudostaurosira pseudoconstruens*. Diversity in zone 2 exhibits a rather stable, high profile
240 flora, dominated by *P. brevistriata*, *P. pseudoconstruens* and *P. bodanica*, while
241 *Gomphonema olivaceoides* and *Karayevia suchlandtii* appear in the record for the first time
242 at c. 1400 and 1070 cal yrs BP, respectively. Motile diatoms become persistently lower than
243 the mean at this time during zone 2, while low profile diatom abundances increase to
244 fluctuate about the average (Fig 4). Zone 3 occurs just before a major change in diatom
245 composition (PCA-1) and beta-diversity (Fig 3). Several species decline from the record
246 altogether including *S. exiguiformis* and *H. schmassmannii*, while other species reach peak
247 abundance for the whole profile, including *P. bodanica* and *G. olivaceoides*, and diatoms
248 which occupy low profile guild status in general (Fig 4). *Denticula subtilis* appears in the
249 record for the first time at c. 400 cal yrs BP. During zone 3, low profile and planktic diatoms
250 increase to their highest values for the whole record, while profile diatoms are persistently



251 lower than the mean. Diatom fluxes range from 0.07 – 7.02 (mean 1.85) valves $\times 10^6$ cm^{-2} yr

252 ¹. When centred around the mean, fluxes are highest in zone 2, between c. 1500 - 800 cal

253 yrs BP (450 – 1150 CE), but decline at c. 800 cal yrs BP (1150 CE), to lowest values from c.

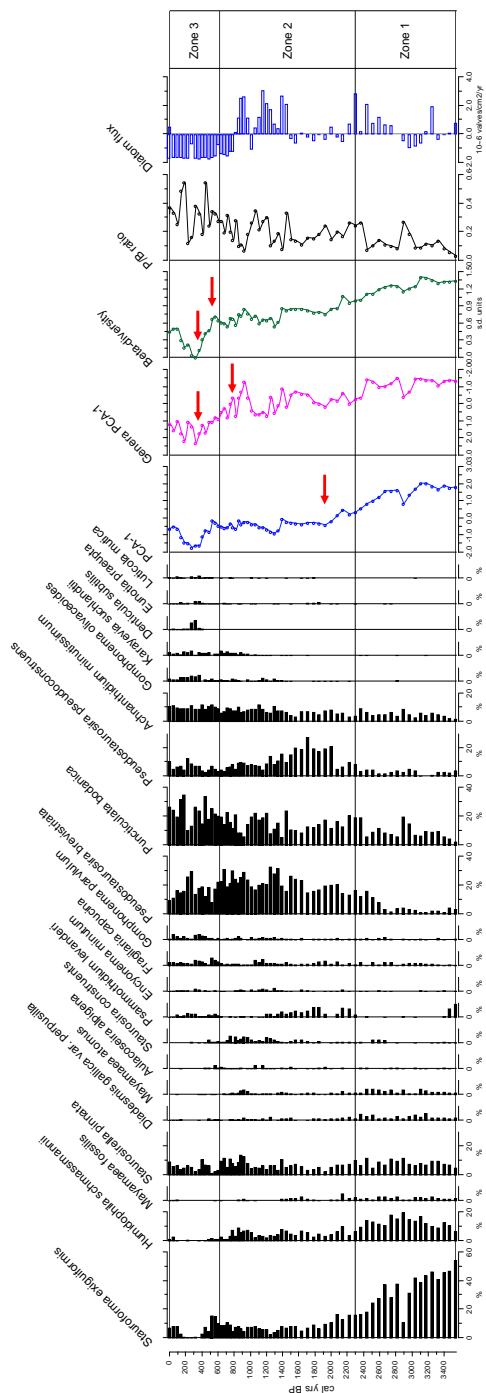
254 600 cal yrs BP (1350 CE) to the present (Fig 3).

255

256 **Figure 3:** Diatoms shown greater than 3% in more than one sample. Diatom species are
257 given as relative abundances. Also shown are PCA axes 1 scores for species and genera,
258 beta-diversity values, planktonic-benthic (P/B) ratio data, and mean-centred diatom fluxes.
259 Zones were delimited using CONISS – see text for details. Red arrows delineate important
260 breakpoints in data (where $p < 0.001$). [see below]

261

262

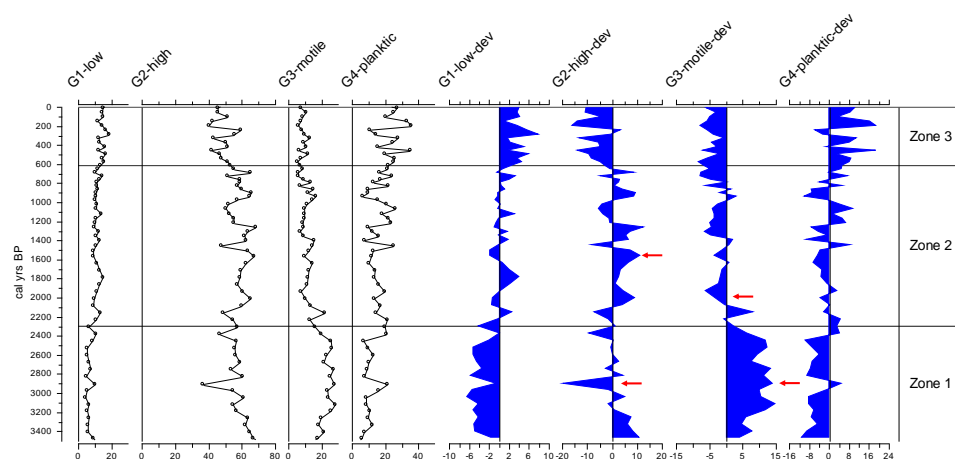


263
264
265



266
267
268
269
270
271
272

Figure 4: All diatoms were classified into one of four guilds (after Passy 2007, and Rimet and Bouchez 2012): low profile (guild 1), high profile (guild 2), motile (guild 3) and planktic (guild 4). Guilds are presented as relative abundances to the left, and deviations around the mean to the right. Red arrows delineate important breakpoints in data (where $p < 0.001$).

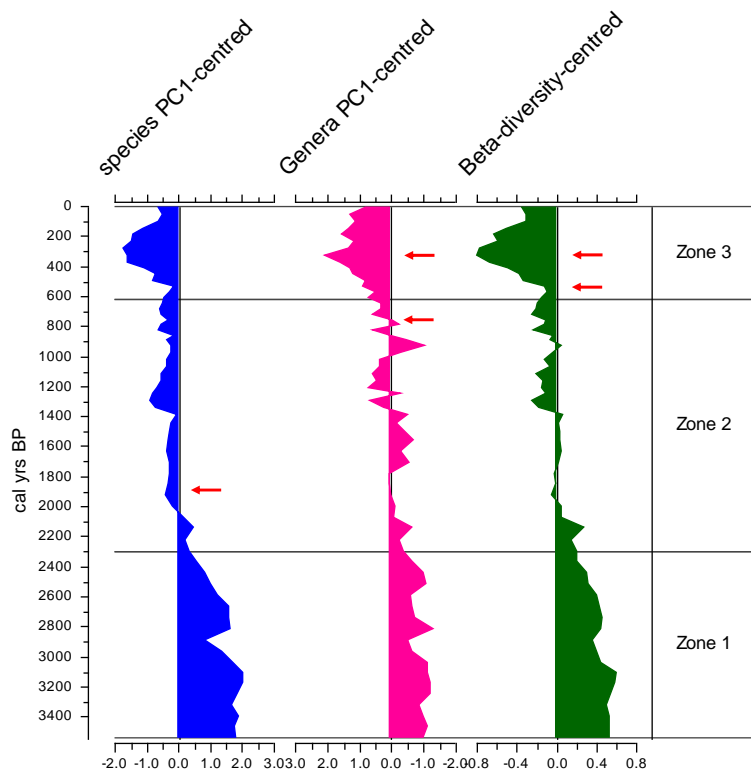


273
274
275
276
277
278
279
280
281
282
283
284
285
286
287
288

PCA highlights a very strong first axis gradient which accounts for over 45% of variation in the diatom data. Trends in PCA-1 are most clearly seen in Fig 5, as deviations around the mean. Breakpoint analysis indicates major ($p < 0.001$) change in PCA axis 1 scores (Table 2), close to the transition when PCA values switch from being higher than the mean, to being lower than the mean, and low values persist for the rest of the record. Genera PCA axis 1 scores exhibit a permanent shift to lower-than-mean scores at c. 800 yrs BP (Fig 5). Beta-diversity (estimated from DCCA; 1.033 SD units) shows a similar pattern to PCA-1, with breakpoints identified at c. 515 cal yr BP \pm 40 years, and 335 cal yr BP \pm 33 years (Table 2; Fig 5).



289 **Figure 5:** Ordination and biodiversity trends shown as deviations around the mean. Red
 290 arrows delineate important breakpoints in data (where $p < 0.001$).
 291



292

293

294 Table 2: Significant breakpoints in diatom trend data; $p < 0.001$).

295

	Breakpoint 1	p value	Breakpoint 2	p value
Species PCA	1850 BP \pm 200	$p < 0.001$	none	
Genera PCA	760 BP (1190 CE) \pm 85	$p < 0.001$	330 BP (1620 CE) \pm 70	$p < 0.001$
Beta-diversity	515 BP (1435 CE) \pm 97	$p < 0.001$	335 BP (1615 CE) \pm 33	$p < 0.001$
Guild 2 – High profile	2910 BP \pm 127	$p < 0.001$	1565 BP \pm 175	$p < 0.001$
Guild 3 – Motile	2880 BP \pm 69	$p < 0.001$	1960 BP \pm 128	$p < 0.001$

296

297



298

299 **4. Discussion:**

300

301 **4.1 Neoglacial trends in diatom diversity**

302 For much of the past 3,500 years, the diatom flora in Lake Yuhuang Chi was dominated by
303 species in the Fragilariaceae (Fig 3), which are common in high altitude lakes. Fragilarioids
304 are often opportunistic, growing well in lakes with a short growing season and long periods
305 of ice cover (e.g. Lotter and Bigler 2000). For example, July air temperature and ice cover
306 duration have both been shown to have significant influence on fragilarioids in the European
307 Alps (Schmidt et al. 2004), while in a sub-alpine lake in the Eastern Sayan mountains,
308 insolation and northern hemisphere air temperatures played a strong role on modulating
309 fragilarioid responses through the Holocene (Mackay et al. 2012). The abundant, high profile
310 species *S. exiguiformis*, is common in dystrophic lakes, which have high concentrations of
311 humic acids (Flower et al. 1996). Allochthonous provision of humic acids can provide
312 essential resources to lakes. The decline in *S. exiguiformis* may be indicative of Lake
313 Yuhuang Chi becoming less dystrophic, perhaps due to less dissolved organic matter being
314 transported into the lake. Zhou et al. (2010) demonstrate a shift from deciduous-conifer
315 mixed forest to steppe forest from elsewhere in the Qinling Mountains, especially after
316 2,900 cal yrs BP, which will have altered catchment – lake dynamics and the transport of
317 allochthonous material. This coincides with breakpoints for both high guild (guild 2) and
318 motile (guild 3) diatoms (Table 2), which may be related to the provision of resources linked
319 to catchment changes around the lake.

320

321 The number of limiting resources has a defining influence on community composition. In
322 aquatic environments, when the number of limiting resources increases during times of
323 environmental stress, deterministic processes become more important in structuring
324 communities, leading to a decline in beta-diversity (Chase 2010; Larson et al. 2016). Initially,
325 beta-diversity between 3,500 – 3,100 cal yrs BP does not decline (Fig 3), which suggests



326 that at the start of our record, diatoms were able to adapt to changing resources, such that
327 resources were not limiting. The presence of *H. schmassmannii* (a motile diatom) in alpine
328 and arctic lakes is linked to relatively low levels of DOC (Buczko et al. 2015). In Lake
329 Yuhuang Chi, therefore, the initial increase of this species suggests that it replacing *S.*
330 *exiguiformis* as resources into the lake changed. The decline in this species after c. 2800 cal
331 yrs BP tracks the switch to steppe forest (Zhou et al. 2010) and the progressively cooler and
332 more arid climate (Wang et al. 2005; Chen et al. 2015b). Declining beta-diversity (especially
333 during the latter stages of zone 1, after 2,800 cal yrs BP), suggests that as regional
334 temperatures cooled and aridity increased (Chen et al. 2015a), resources became more
335 limiting (Fig 6a).

336

337 However, there were periods when the availability of resources stabilised or even increased
338 slightly during the neoglacial, e.g. between c. 2,000 – 1,400 cal yrs BP (Fig 6a). This period
339 coincides with distinctly warmer Arctic and European temperatures (PAGES 2k Consortium
340 2013), commonly referred to as the 'Roman Warm Period', although in eastern China
341 temperatures declined, especially due to strong winter temperature anomalies (Ge et al.
342 2003). Strong seasonality at this time therefore likely affected resource availability, given
343 that high profile diatoms dominate the assemblage, and exhibit a significant breakpoint at c.
344 1565 cal yrs BP (Table 2; Fig 4).

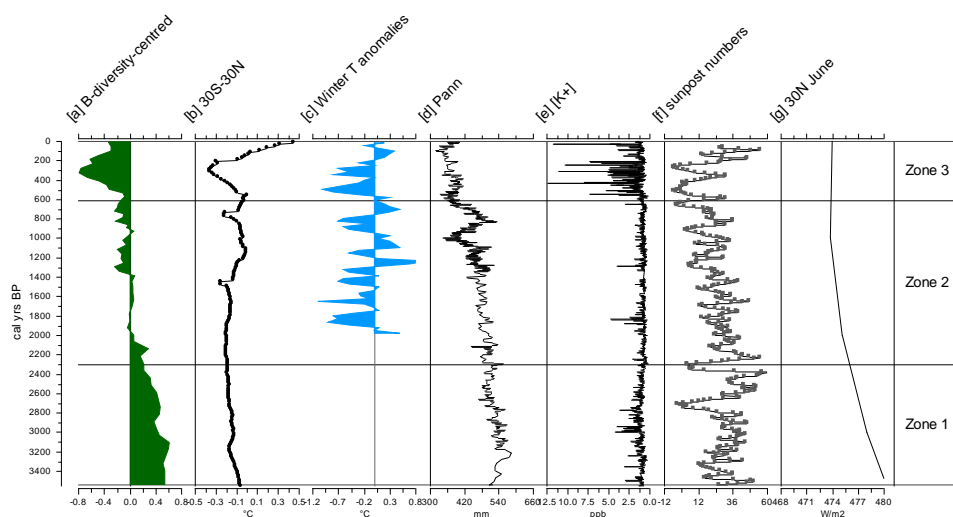
345

346



347

348 **Figure 6:** Beta-diversity here is plotted alongside internal and external climate forcings:
349 mean temperature stack records for low latitude temperature anomalies (Fig 7b; Marcott et
350 al. 2013); Chinese winter temperature anomalies (Fig 7c; Ge et al. 2003); trends in pollen-
351 inferred mean annual precipitation (Fig 7d; Chen et al. 2015a); K⁺ concentrations in the
352 GISP ice core (Fig 7e; Mayewski et al. 2004); sun spot numbers (Fig 7f; Solanki et al. 2004);
353 June solar insolation at 30 N (W m⁻²) (Fig 7g; Berger and Loutre 1991)
354



355

356

357 Between 1400 – 615 cal yrs BP (550 - 1335 CE), beta-diversity was lower than average
358 (Fig 6a), and quite variable. Temperature reconstructions from over 200 tree-ring records in
359 Asia reveal a period of greater warmth than the following four centuries (PAGES 2k
360 Consortium 2013), including central China (Ge et al. 2003) (Fig 6c). Precipitation in central
361 China is closely tied to the intensity of the Asian summer monsoon (ASM) (Chen et al.
362 2015a), and monsoon strength showed distinct variability, being higher in central (Paulsen
363 et al. 2003; Chen et al. 2015b; Wang et al. 2016) and north east China (Chen et al. 2015a,b)
364 than north west China (Chen et al. 2015b). This period coincides with the Medieval Climatic
365 Anomaly (MCA), sometimes referred to the Medieval Warm Period. Sub-decadal isotopic
366 records from a stalagmite from Buddha cave in the Qinling Mountains indicate a period of
367 warm, wet climate between c. 985 – 475 cal yrs BP (965 – 1475 CE) (Paulsen et al. 2003),



368 while phenology records from the Yellow and Yangtze rivers show that winter half-year
369 temperatures were high between 1380 – 640 cal yrs BP (570 – 1310 CE) (Ge et al. 2003;
370 Fig 6c). A recent palaeolimnological investigation from another alpine lake on Taibai
371 Mountain, Lake Sanqing Chi, inferred warm, wet conditions due to increased presence of
372 *Quercus* and *Betula* pollen (Wang et al. 2016), while Li et al. 2005 used pollen evidence to
373 show that the warmest period in the late Holocene on Tabai mountain occurred between 520
374 – 1220 CE, with temperatures perhaps being as much as 2 °C warmer than mean annual
375 temperatures observed today.

376

377 In oligotrophic lakes, growth of the planktic diatom *P. bodanica* is related to increased mixing
378 depth (Saros and Anderson 2015), because it can tolerate relatively low light levels and take
379 advantage of increased nutrient availability (Malik and Saros 2016). Increasing diatom flux at
380 Lake Yuhuang Chi between c. 1500 - 800 cal yrs BP (450 – 1150 CE) (driven mainly by
381 increasing *P. bodanica*), likely reflects shorter ice duration, with enhanced overturn, driven
382 by increased summer monsoon intensity (Chen et al. 2015a). An increase in beta-diversity
383 reflects the decline in the number of resources that are limited. However, these changes at
384 Lake Yuhuang Chi are relatively muted in comparison to the almost complete switch in
385 oligotrophic to eutrophic diatom communities at the high altitude Gonghai Lake (1,840
386 m.a.s.l.), located to the north west in the Chinese Loess Plateau. Differences are likely due
387 to the altitudinal differences and phosphorus-rich erodible soils of the loess catchment (Liu
388 et al. 2017).

389

390 **4.2 Abrupt ecological change during centennial-scale cold events**

391 Against a backdrop of low northern hemisphere summer insolation (Fig 6g), amplified by
392 centennial-scale oceanic variability (Renssen *et al.*, 2006), late Holocene cold events were
393 caused by several “overlapping” factors (such as volcanic eruptions and solar minima) (e.g.
394 Wanner *et al.*, 2014). The most recent wide-scale cold event is the period commonly known
395 as the Little Ice Age approximately 1400 – 1850 CE, caused by several interacting, time-



396 transgressive forcings. It is the cooling event that we focus on in this study, because cluster
397 analyses of diatom assemblages delineate the boundary between zones 2 and 3 at 1335
398 CE, and beta-diversity significantly declines at this time to lowest values in the whole record
399 by 1615-1620 CE (Fig 3, Fig 6a).

400

401 Describing the Little Ice Age as a period characterised by cooler climate and glacier
402 readvance is rather simplistic, but one that has proven quite resilient, even as its
403 complexities are better understood (e.g. Matthews and Briffa 2005). As more regions are
404 investigated, impacts extend to changes in aridity as well as temperature. For example,
405 Chen et al. (2015b) demonstrated that by and large, regions north of 34° latitude (where our
406 study site is located) were generally drier than regions further south, with the extent of aridity
407 being affected by ocean-atmospheric interactions, such as ENSO, and its teleconnections to
408 SE Asia. The LIA is especially characterised by a strengthened Siberian High (SH), a semi-
409 permanent anticyclone centred over Eurasia which strengthens intensively every winter. A
410 strong Siberian High results in a strong East Asian Winter Monsoon (EAWM) (Zhang et al.
411 1997). K⁺ concentrations in the GISP ice core clearly show that the Siberian High was
412 especially strong between 1400 – 1800 CE (Fig 6f; Mayewski et al. 2004). Concurrent with
413 increased aridity, global low latitude temperature records show rapid cooling at this time (Fig
414 6b; Marcott et al. 2013), which in China led to very low winter anomalies from phenological
415 records (Ge et al. 2003) (Fig 6c).

416

417 Very low diatom fluxes characterise the past 800 years at Lake Yuhuang Chi (Fig 3),
418 indicative of reduced diatom productivity, linked to prevailing colder climate. During this time,
419 low profile and planktic diatom guilds are relatively the most important they've been for the
420 past 3500 years (Fig 4), indicating that conditions which caused the lake to become
421 oligotrophic 800 years ago, still persist today. However, planktonic diatoms show a distinct
422 decline during the LIA, likely related to extreme cold conditions and extended ice cover on
423 the lake. The disappearance of *S. exiguiformis* from the record may be due to enhanced



424 frozen soils, leading to the cessation of carbon transport to the lake, while the
425 disappearance of *H. schamassmannii* may be because it cannot tolerate such low water
426 temperatures (Buczko et al. 2015). The appearance of *Denticula subtilis*, a very motile
427 diatom that can also be an epiphyte commonly found growing on mosses in littoral habitats,
428 may be due to its exploiting a new habitat for the limited resources available. It may also be
429 reflective of the lake becoming more shallow due to increased aridity; precipitation minima
430 were reconstructed from nearby by Gonghai lake (Chen et al. 2015a). At neighbouring Lake
431 Sanqing Chi, pollen frequencies from *Larix* and *Ephedra* are very high, indicative of cold, dry
432 conditions (Wang et al. 2016). Following harshest conditions for diatom growth in Lake
433 Yuhuang Chi in the middle of the 17th century, beta-diversity increases once more, indicative
434 of more resources becoming available, although diatom fluxes overall remain very low.
435 Modern tundra vegetation developed again on Tabai, with the establishment of the modern
436 tree-line (Li et al. 2005).

437

438 While cold and arid climate during the LIA had a major impact on diatom diversity in Lake
439 Yuhuang Chi, impacts from previous centennial-scale cold events such as the 2,800 yr BP
440 event, are inconclusive. Like the LIA, the event dated at c. 2,800 yr BP is concurrent with a
441 deep, abrupt reduction in solar activity (Fig 6f), which led to a decline in surface water
442 temperatures in the North Atlantic (Andersson *et al.*, 2003), weaker meridional overturning
443 circulation (Hall *et al.*, 2004) and sea-ice expansion (Renssen et al. 2006). But although
444 these events led to a rapid weakening in ASM intensity in southern China (Wang et al.
445 2005), reconstructed precipitation from Gonghai Lake in northern China suggests that aridity
446 was already declining from c. 3,100 cal yrs BP (Fig 6d) (Chen et al. 2015b). Moreover, there
447 is a distinct difference in GISP2 K⁺ concentrations, which suggests that the Siberian High
448 around the time of the did not reach the strengths observed during the LIA (Fig 6e). At Lake
449 Yuhuang Chi, while there are small declines in beta-diversity and total diatom fluxes, these
450 occur c. 3000 cal yrs BP, in line with increasing regional aridity (Chen et al. 2015b).
451 Breakpoints in high profile and motile diatom guilds are detected slightly later at c. 2,900 cal



452 yrs BP. The difference in expression of these cold events at Lake Yuhuang Chi highlights
453 their uneven impacts globally.

454

455 **5. Conclusions**

456

457 Trends in diatom beta-diversity in freshwater ecosystems in the Qinling mountains of central
458 China reflect changing resource availability, linked to both long term, and abrupt, climate
459 change impacts on lakes and their catchments. For example, the overall gradual decline in
460 beta-diversity over the past 3,500 years mirrors declining low latitude June insolation, which
461 drives overall low latitude cooling (Marcott et al. 2013). This suggests a strong link between
462 orbitally-forced climate change and the availability of limiting resources in this biodiversity-
463 rich alpine region. Over the last 1300 years, impacts related to the Medieval Climatic
464 Anomaly and the Little Ice Age are also expressed in palaeolimnological records from Lake
465 Yuhuang Chi. Inferred increased summer precipitation during the MCA from nearby records
466 resulted in increased diatom fluxes, including planktonic species adapted to mixing of deep
467 waters. Colder, more arid conditions during the Little Ice Age period had an impact on
468 freshwater ecosystem dynamics, providing evidence that this alpine region in central China
469 is very sensitive to climate change, caused by both extrinsic and intrinsic factors. Regional
470 warming after the LIA led to more resources being made available to diatoms once more,
471 especially planktonic species, although overall diatom fluxes remain low compared to earlier
472 periods.

473

474 **6. Author contribution**

475

476 BC & JC designed the study. BC undertook the diatom analyses, and AZ the radiocarbon
477 dating. JA provided assistance with statistical analyses, and AWM prepared the manuscript
478 with contributions from all authors.

479



480 **7. Acknowledgements:**

481

482 Funding: The work was supported by a China Scholarship Council award to Dr Bo Cheng,

483 and by the National Natural Science Foundation of China (Grants No. 41771208; No.

484 41790421). The authors declare that they have no conflict of interest.

485



486

487 **8. References**

488

489 Andersson, C., Risebrobakken, B., Jansen, E., and Dahl, S. O.: Late Holocene surface
490 ocean conditions of the Norwegian Sea (Vøring Plateau), *Paleoceanography*, 18, 1044,
491 doi:10.1029/2001PA000654, 2003.

492

493 Birks, H. J. B.: Estimating the amount of compositional change in late-Quaternary pollen-
494 stratigraphical data, *Veg. Hist. Archaeobot.*, 16, 197-202, 2007.

495

496 Blaauw, M.: Methods and code for 'classical' age-modelling of radiocarbon
497 sequences, *Quat. Geochron.*, 5, 512-518, 2010.

498

499 Buytaert, W., Moulds, S., Acosta, L., De Bievre, B., Olmos, C., Villacis, M., Tovar, C.,
500 and Verbist, K. M. J.: Glacial melt content of water use in the tropical Andes, *Environ.*
501 *Res. Lett.*, 12, 114014, 2017.

502

503 Buczkó, K., Wojtal, A. Z., Beszteri, B., and Magyari, E. K.: Morphology and distribution of
504 *Navicula schmassmannii* and its transfer to genus *Humidophila*, *Studia Botanica*
505 *Hungarica*, 46, 25-41, 2015.

506

507 Chase, J. M.: Drought mediates the importance of stochastic community assembly, *P.*
508 *Natl. Acad. Sci. USA*, 104, 17430-17434, 2010.

509

510 Chen, F., Xu, Q., Chen, J., Birks, H. J. B., Liu, J., Zhang, S., Jin, L., An, C., Telford, R. J.,
511 Cao, X., and Wang, Z.: East Asian summer monsoon precipitation variability since the
512 last deglaciation, *Sci. Rep. UK*, 5, 11186, 2015a.

513



- 514 Chen, J., Chen, F., Feng, S., Huang, W., Liu, J., and Zhou, A.: Hydroclimatic changes in
515 China and surroundings during the Medieval Climate Anomaly and Little Ice Age: spatial
516 patterns and possible mechanisms, *Quaternary Sci. Rev.*, 107, 98-111, 2015b.
517
- 518 Cook, E. R., Krusic, P. J., Anchukaitis, K. J., Buckley, B. M., Nakatsuka, T., Sano, M.,
519 and PAGES Asia2k Members: Tree-ring reconstructed summer temperature anomalies
520 for temperate East Asia since 800 C.E., *Clim. Dynam.*, 41, 2957-2972, 2013.
521
- 522 Cook, E. R., Anchukaitis, K. J., Buckley, B. M., D'Arrigo, R. D., Jacoby, G. C., and
523 Wright, W. E.: Asian monsoon failure and megadrought during the last
524 millennium, *Science*, 328, 486-489, 2010.
525
- 526 Fan, J. T., Li, J. S., Xia, R., Hu, L. L., Wu, X. P., and Guo, L.: Assessing the impact of
527 climate change on the habitat distribution of the giant panda in the Qinling Mountains of
528 China, *Ecol. Model.*, 274, 12–20, 2014.
529
- 530 Flower, R. J., Jones, V. J., and Round, F. E.: The distribution and classification of the
531 problematic *Fragilaria (virescens V.) exigua* Grun./*Fragilaria exiguiformis* (Grun.) Lange-
532 Bertalot: A new species or a new genus?, *Diatom Res.*, 11, 41–57. 1996.
533
- 534 Ge, Q., Zheng, J., Fang, X., Man, Z., Zhang, Z., Zhang, P., and Wang, W.: Winter half-
535 year temperature reconstruction for the middle and lower reaches of the Yellow River
536 and Yangtze River, China, during the past 2000 years, *Holocene*, 13, 933-940, 2003.
537
- 538 Grêt-Regamey, A., Brunner, S. H., and Kienast, F.: Mountain ecosystem services: who
539 cares?, *Mt. Res. Dev.*, 32, S23-S34, 2012.
540



- 541 Guo, J., Huang, G., Wang, X., Li, Y., and Lin, Q.: Investigating future precipitation
542 changes over China through a high-resolution regional climate model ensemble, *Earth's*
543 *Future*, 5, 285-303, 2017.
- 544
- 545 Hall, I. R., Bianchi, G. G., and Evans, J. R.: Centennial to millennial scale Holocene
546 climate-deep water linkage in the North Atlantic, *Quaternary Sci. Rev.*, 23, 1529–1536,
547 2004.
- 548
- 549 Juggins, S.: rioja: Analysis of Quaternary Science Data, R package version
550 3.5.1. <http://cran.r-project.org/package=rioja>, 2017.
- 551
- 552 Krammer, K., and Lange-Bertalot, H.: Bacillariophyceae: Naviculaceae. In: Ettl, H.,
553 Gerloff, J., Heynig, H., Mollenhauer, D. (Eds.), *Süßwasserflora von Mitteleuropa*. Band
554 2, Teil 1. Gustav Fischer, Stuttgart, 1986.
- 555
- 556 Krammer, K., and Lange-Bertalot, H.: Bacillariophyceae: Bacillariaceae, Epithemiaceae,
557 Surirellaceae. In: Ettl, H., Gerloff, J., Heynig, H., Mollenhauer, D. (Eds.), *Süßwasserflora*
558 *von Mitteleuropa*. Band 2, Teil 2. Gustav Fischer, Stuttgart, 1988.
- 559
- 560 Krammer, K., and Lange-Bertalot, H.: Bacillariophyceae: Achnantheaceae, Kritische Erga-
561 nzungen zu Navicula (Lineolatae) und Gomphonema Gesamtliteraturverzeichnis. In: Ettl,
562 H., Gerloff, J., Heynig, H., Mollenhauer, D. (Eds.), *Süßwasserflora von Mitteleuropa*.
563 Band 2, Teil 4. Gustav Fischer, Stuttgart, 1991a.
- 564
- 565 Krammer, K., and Lange-Bertalot, H.: Bacillariophyceae: Centrales, Fragilariaceae,
566 Eunotiaceae. In: Ettl, H., Gerloff, J., Heynig, H., Mollenhauer, D. (Eds.), *Süßwasserflora*
567 *von Mitteleuropa*. Band 2, Teil 3. Gustav Fischer, Stuttgart, 1991b.
- 568



- 569 Lange-Bertalot, H.: Diatoms of Europe, Volume 2: *Navicula* sensu stricto. 10 genera
570 separated from *Navicula* sensu lato *Frustulia*. In: Lange- Bertalot, H. (Ed.) Diatoms of
571 Europe: diatoms of the European inland waters and comparable habitats. A.R.G.
572 Gantner Verlag K.G., Ruggell, Germany, 2001.
573
- 574 Larson, C. A., Adumatioge, L., and Passy, S. I.: The number of limiting resources in the
575 environment controls the temporal diversity patterns in the algal benthos, *Microbial*
576 *Ecol.*, 72, 64-69, 2016.
577
- 578 Leprieur, F., Tedesco, P. A., Hugueny, B., Beauchard, O., Dürr, H. H., Brosse, S., and
579 Oberdorff, T.: Partitioning global patterns of freshwater fish beta diversity reveals
580 contrasting signatures of past climate changes, *Ecol. Lett.*, 14, 325–334, 2011.
581
- 582 Li, X., Dodson, J., Zhou, J., Wang, S., and Sun, Q.: Vegetation and climate variations at
583 Taibai, Qinling Mountains in central China for the last 3500 cal BP, *Journal Integr. Plant*
584 *Biol.*, 47, 905-916, 2005.
585
- 586 Liu, H., Tang, Z., Dai, J., Tang, Y., and Cui, H.: Larch timberline and its development in
587 North China. *Mt. Res. Dev.*, 22, 359-367, 2002.
588
- 589 Liu, J., Rühland, K. M., Chen, J., Xu, Y., Chen, S., Chen, Q., Huang, W., Xu, Q., Chen,
590 F., and Smol, J. P.: Aerosol-weakened summer monsoons decrease lake fertilization on
591 the Chinese Loess Plateau, *Nat. Clim. Change*, 7, 190-195, 2017.
592
- 593 Lotter, A. F., and Bigler, C.: Do diatoms in the Swiss Alps reflect the length of ice cover,
594 *Aquat. Sci.*, 62, 125-141, 2000.
595



- 596 Mackay, A. W., Bezrukova, E. V., Leng, M. J., Meaney, M., Nunes, A., Piotrowska, N.,
597 Self, A., Shchetnikov, A., Shilland, E., Tarasov, P., Wang, L., and White, D.: Aquatic
598 ecosystem responses to Holocene climate change and biome development in boreal,
599 central Asia, *Quaternary Sci. Rev.*, 41, 119-131, 2012.
- 600
- 601 Malik, H. I., and Saros, J. E.: Effects of temperature, light and nutrients on five *Cyclotella*
602 sensu lato taxa assessed with in situ experiments in arctic lakes. *J. Plankton Res.*, 38,
603 431-442, 2016.
- 604
- 605 Mann, M. E., Zhang, Z., Rutherford, S., Bradley, R. S., Hughes, M. K., Shindell, D.,
606 Ammann, C., and Faluvegi, G., Ni, F.: Global signatures and dynamical origins of the
607 Little Ice Age and Medieval Climate Anomaly, *Science*, 326, 1256-1260, 2009.
- 608
- 609 Marcott, S. A., Shakun, J. D., Clark, P. U., and Mix, A. C.: A reconstruction of regional
610 and global temperature for the past 11,300 years, *Science*, 339, 1198-1201, 2013.
- 611
- 612 Matthews, J. A., and Briffa, K. R.: The 'Little Ice Age': re-evaluation of an evolving
613 concept, *Geogr. Ann. A.*, 87, 7-36, 2005.
- 614
- 615 Mayewski, P. A., Rohling, E. E., Stager, J. C. et al.: Holocene climate variability,
616 *Quaternary Res.*, 62, 243–255, 2004.
- 617
- 618 Messerli, B., Viviroli, D., and Weingartner, R.: Mountains of the world: vulnerable water
619 towers for the 21st century, *Ambio*, 29-34, 2004.
- 620
- 621 Mori, A. S., Isbell, F., and Seidl, R.: β -Diversity, Community Assembly, and Ecosystem
622 Functioning, *Trends Ecol. Evol.*, 33, 549-564, 2018.



623

624 Muggeo, V. M. R.: Segmented: An R Package to Fit Regression Models with Broken-
625 Line Relationships, *R News*, 8, 20-25, 2008.

626

627 PAGES 2k Consortium: Continental-scale temperature variability during the
628 past two millennia, *Nat. Geosci.* 6, 339e346, 2013.

629

630 Passy, S. I.: Diatom ecological guilds display distinct and predictable behaviour along
631 nutrient and disturbance gradients in running waters, *Aquat. Bot.*, 86, 171–178, 2007.

632

633 Paulsen, D. E., Li, H. C., and Ku, T. L.: Climate variability in central China over the last
634 1270 years revealed by high-resolution stalagmite records, *Quaternary Sci. Rev.*, 22,
635 691-701, 2003.

636

637 Pepin, N., Bradley, R. S., Diaz, H. F., Baraër, M., Caceres, E. B., Forsythe, N., Fowler,
638 H., Greenwood, G., Hashmi, M. Z., Liu, X. D., and Miller, J. R.: Elevation-dependent
639 warming in mountain regions of the world, *Nat. Clim. Change*, 5, 424-430, 2015.

640

641 Reimer, P. J., Bard, E., Bayliss, A. et al.: IntCal13 and Marine13 radiocarbon age
642 calibration curves 0–50,000 years cal BP. *Radiocarbon*, 55, 1869–1887, 2013.

643

644 Renssen, H., Goosse, H., and Muscheler, R.: Coupled climate model simulation of
645 Holocene cooling events: oceanic feedback amplifies solar forcing, *Clim. Past*, 2, 79-90,
646 2006.

647

648 Rimet, F., and Bouchez, A.: Life-forms, cell-sizes and ecological guilds of diatoms in
649 European rivers, *Knowl. Manag. Aquat. Ecosyst.* 406, 01, 2012.

650



651 Saros, J. E., and Anderson, N. J. The ecology of the planktonic diatom *Cyclotella* and its
652 implications for global environmental change studies, *Biol. Rev.*, 90, 522-541, 2015.

653

654 Schmidt, R., Kamenik, C., Lange-Bertalot, H., and Klee, R.: *Fragilaria* and *Staurosira*
655 (*Bacillariophyceae*) from sediment surfaces of 40 lakes in the Austrian Alps in relation
656 to environmental variables, and their potential for palaeoclimatology. *J. Limnol.*, 63, 171–
657 189, 2004.

658

659 Solanki, S. K., Usoskin, I. G., Kromer, B., Schüssler, M., and Beer, J: An unusually active
660 sun during recent decades compared to the previous 11,000 years, *Nature*, 431, 1084–
661 1087, 2004.

662

663 Šmilauer, P., and Lepš, J.: *Multivariate analysis of ecological data using CANOCO 5*.
664 Cambridge University Press. 2014.

665

666 Smol, J. P., Wolfe, A. P., Birks, H. J. B., et al.: Climate-driven regime shifts in the
667 biological communities of arctic lakes, *P. Natl. Acad. Sci. USA*, 102, 4397-4402, 2005.

668

669 Tan, L., Cai, Y., An, Z., Yi, L., Zhang, H., and Qin, S.: Climate patterns in north central
670 China during the last 1800 yr and their possible driving force, *Clim. Past*, 7, 685-692,
671 2011.

672

673 Tan, L., Cai, Y., Cheng, H., Edwards, E. R., Gao, Y., Xu, H., Zhang, H., and An, Z.:
674 Centennial- to decadal-scale monsoon precipitation variations in the upper Hanjiang
675 River region, China over the past 6650 years, *Earth Planet. Sci. Lett.*, 482, 580-590,
676 2018.

677



- 678 Wang, Y., Cheng, H., Edwards, R. L., He, Y., Kong, X., An, Z., Wu, J., Kelly, M. J.,
679 Dykoski, C. A., and Li, X.: The Holocene Asian monsoon: links to solar changes and
680 North Atlantic climate, *Science*, 308, 854-857, 2005.
- 681
682 Wang, H., Song, Y. Cheng, Y., Luo, Y., Gao, Y., Deng, L., and Liu, H.: Mineral
683 magnetism and other characteristics of sediments from a sub-alpine lake (3080 m asl) in
684 central east China and their implications on environmental changes for the last 5770
685 years, *Earth Planet. Sci. Lett.*, 452, 44-59, 2016.
- 686
687 Wanner, H., Mercolli, L., Grosjean, M., and Ritz, S.P.: Holocene climate variability and
688 change: a database review, *J. Geol. Soc. Lond.*, 172, 254-263, 2014.
- 689
690 Williams, D. M., and Round, F. E.: Revision of the genus *Fragilaria*. *Diatom Res.*, 2, 267-
691 288, 1987.
- 692
693 Yan, L., and Liu, X.: Has climatic warming over the Tibetan Plateau paused or continued
694 in recent years? *J. Earth, Ocean Atmos. Sci.*, 1, 13-28, 2014.
- 695
696 Yang, W., Yan, Y., Zhang, Y., Guo, W., and Zha, F.: Geoheritages in the Qinling
697 Orogenic Belt of China: Features and comparative analyses, *Geol. J.*, 53, 98-413, 2018.
- 698
699 Zhang, Y., Sperber, K. R., and Boyle, J. S.: Climatology and interannual variation of the
700 east Asian winter monsoon: Results from the 1979–95 NCEP/NCAR reanalysis, *Mon.*
701 *Wea. Rev.*, 125, 2605–2619, 1997.
- 702
703 Zhang, Y. B., Wang, Y. Z., Phillips, N., Ma, K. P., Li, J. S., and Wang, W.: Integrated
704 maps of biodiversity in the Qinling Mountains of China for expanding protected
705 areas. *Biol. Conserv.*, 210, 64-71, 2017.



706

707 Zhou, A., Sun, H., Chen, F., Zhao, Y., An, C., Dong, G., Wang, Z., and Chen, J.: High-

708 resolution climate change in mid-late Holocene on Tianchi Lake, Liupan Mountain in the

709 Loess Plateau in central China and its significance. Chinese Sci. Bull., 55, 2118-2121,

710 2010.

711



712

713 **Figure Legends**

714

715 Figure 1: Regional position of Lake Yuhuang Chi in the Qinling Mountains of central Asia.

716 The lake is situated 3365m asl, and was formed by glacial activity. The photograph of the

717 frozen lake to the right shows the small catchment and tundra vegetation.

718

719 Figure 2: The age model determined on 5 radiocarbon dates of organic bulk sediments from

720 core YHC15A. The age-depth model was developed with smooth fitting using CLAM 2.2

721 (Blaauw, 2010).

722

723 Figure 3: Diatoms shown greater than 3% in more than one sample. Diatom species are

724 given as relative abundances. Also shown are PCA axes 1 scores for species and genera,

725 beta-diversity values, planktonic-benthic (P/B) ratio data, and mean-centred diatom fluxes.

726 Zones were delimited using CONISS – see text for details. Red arrows delineate important

727 breakpoints in data (where $p < 0.001$).

728

729 Figure 4: All diatoms were classified into one of four guilds (after Passy 2007, and Rimet and

730 Bouchez 2012): low profile (guild 1), high profile (guild 2), motile (guild 3) and planktic (guild

731 4). Guilds are presented as relative abundances to the left, and deviations around the mean

732 to the right. Red arrows delineate important breakpoints in data (where $p < 0.001$).

733

734 Figure 5: Ordination and biodiversity trends shown as deviations around the mean. Red

735 arrows delineate important breakpoints in data (where $p < 0.001$).

736

737 Figure 6: Beta-diversity here is plotted alongside internal and external climate forcings:

738 mean temperature stack records for low latitude temperature anomalies (Fig 7b; Marcott et

739 al. 2013); Chinese winter temperature anomalies (Fig 7c; Ge et al. 2003); trends in pollen-



740 inferred mean annual precipitation (Fig 7d; Chen et al. 2015a); K⁺ concentrations in the
741 GISP ice core (Fig 7e; Mayewski et al. 2004); sun spot numbers (Fig 7f; Solanki et al. 2004);
742 June solar insolation at 30 N (W m⁻²) (Fig 7g; Berger and Loutre 1991)
743
744
745